frontiers | Frontiers in Physics

TYPE Brief Research Report
PUBLISHED 07 February 2023
DOI 10.3389/fphy.2023.1116023

OPEN ACCESS

EDITED BY
Aldo Bonasera,
Texas A&M University, United States

REVIEWED BY
Guoqiang Zhang,
Shanghai Advanced Research Institute (CAS), China
Johann Rafelski,
University of Arizona, United States

*CORRESPONDENCE
István Papp,
papp.istvan@wigner.hu

SPECIALTY SECTION
This article was submitted to Nuclear Physics, a section of the journal Frontiers in Physics

RECEIVED 05 December 2022
ACCEPTED 26 January 2023
PUBLISHED 07 February 2023

CITATION
Papp I, Bravina L, Csete M, Kumari A, Mishustin IN, Motornenko A, Rácz P, Satarov LM, Stöcker H, Strottman DD, Szenes A, Vass D, Szokol ÁN, Kámán J, Bonyár A, Biró TS, Csernai LP and Kroó N (2023), Kinetic model of resonant nanoantennas in polymer for laser induced fusion.
Front. Phys. 11:1116023.
doi: 10.3389/fphy.2023.1116023

Kinetic model of resonant nanoantennas in polymer for laser induced fusion

István Papp[1,2]*, Larissa Bravina[3], Mária Csete[1,4], Archana Kumari[1,2], Igor N. Mishustin[5], Anton Motornenko[5], Péter Rácz[1,2], Leonid M. Satarov[5], Horst Stöcker[5,6,7], Daniel D. Strottman[8], András Szenes[1,4], Dávid Vass[1,4], Ágnes Nagyné Szokol[1,2], Judit Kámán[1,2], Attila Bonyár[9], Tamás S. Biró[1,2], László P. Csernai[1,2,5,10,11] and Norbert Kroó[1,2,12] on behalf of (part of NAPLIFE Collaboration)

[1]Wigner Research Centre for Physics, Budapest, Hungary, [2]Hungarian Bureau for Research Development and Innovation, Budapest, Norway, [3]Department of Physics, University of Oslo, Oslo, Norway, [4]Department of Optics and Quantum Electronics, University of Szeged, Szeged, Hungary, [5]Frankfurt Institute for Advanced Studies, Frankfurt/Main, Germany, [6]Institute für Theoretische Physik, Goethe Universität, Frankfurt/Main, Germany, [7]GSI Helmholtzzentrum für Schwerionenforschung GmbH, Darmstadt, Germany, [8]Los Alamos National Laboratory, Los Alamos, NM, United States, [9]Department of Electronics Technology, Faculty of Electrical Engineering and Informatics, Budapest University of Technology and Economics, Budapest, Hungary, [10]Department of Physics and Technology, University of Bergen, Bergen, Norway, [11]Csernai Consult Bergen, Bergen, Norway, [12]Hungarian Academy of Sciences, Budapest, Hungary

Studies of resilience of light-resonant nanoantennas in vacuum are extended to consider the case of polymer embedding. This modifies the nanoantenna's lifetime and resonant laser pulse energy absorption. The effective resonance wavelength is shortened, the peak momentum of resonantly oscillating electrons in the nanorod is reduced by one-third, while the available lifespan of the resonance condition remains the same. This response is expected to strengthen the laser pulse induced nuclear fusion processes. Related numerical simulations were performed using particle-in-cell method in a simulation box of the size 0.223 μm^3, treating the conduction electrons as strongly coupled plasma. In the modeling the polymer background was added with the experimentally measured refractive index of 1.53.

KEYWORDS

partcile-in-cell method, gold nanoparticles, plasmonic effect, polymer, kinetic model

1 Introduction

Recently laser induced fusion with simultaneous volume ignition, a spin-off from relativistic heavy ion collisions, was proposed, where implanted nanoantennas regulated and amplified the light absorption in the fusion target. NAnoPlasmonic Laser Inertial Fusion Experiments (NAPLIFE) [1] is an improved way to achieve laser driven fusion in a non-thermal, collider configuration to avoid instabilities during ignition [2–4]. Targets structured at the nano-scale such as the clusters gas, the nanowire, and the nanohole are also used in laser induced fusion methods as targets [5–8]. It is based on simultaneous (or "time-like") ignition [9, 10], with enhanced energy absorption with the help of nanoantennas implanted into the target material [11]. This should prevent the development of the mechanical Rayleigh-Taylor instability. Furthermore, the nuclear burning should not propagate from a central hot spot to the outside edge as the ignition is simultaneous in the whole volume.

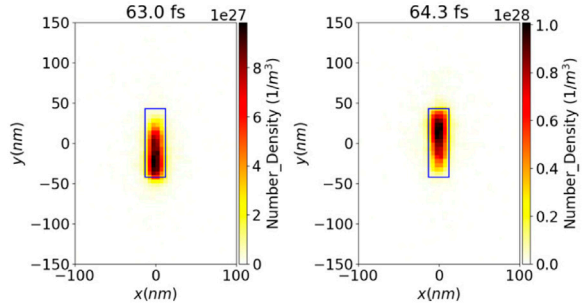

FIGURE 1
(color online) Cross section of the 25 nm (diameter) × 85 nm nanorod showing number density of electrons at the tips, leaving the nanorod at different times *t*, half of the light wave time period apart. The number of electron marker-particles inside the simulation box will decrease with a significant amount by the end of simulation at 120 fs. Light travels from left to right in the *x* direction, the polarization of light is aligned with the nanorod's orientation in *y* direction.

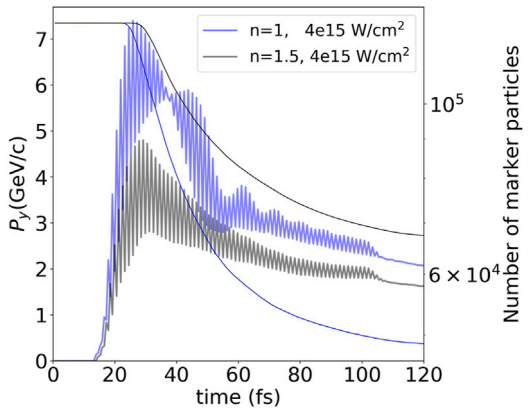

FIGURE 2
(color online) We consider a laser pulse of intensity $I = 4{\cdot}10^{15}$ W/cm^2 and duration of 106 fs. Here we show the time dependence of the total polarity directed momentum of the conducting electrons in the nanorod. The nanorod is in surrounding UDMA-TEGDMA copolymer (black line) and in vacuum (blue line). The UDMA-TEGDMA copolymer decreases the momentum of the emitted (as well as the number of electrons "spilled" out during the process shown by the right axes of the figure) considerably compared to the emission to vacuum. Right axis on the figure shows the number of marker particles still present in the simulation box.

Non-equilibrium and linear colliding configuration have been introduced already [12, 13]. Here we study the idea of layered flat target fuel with embedded nanorod antennas, that regulate laser light absorption to enforce simultaneous ignition. We plan a seven-layer flat target with layer-dependent nanorod densities [14–16]. In order to prepare such a layered target, the ignition fuel (e.g., deuterium, D, tritium, T, or other nuclei for fusion) are embedded into a hard thin polymer material of seven, 3 μm thick layers. These polymers are Urethane Dimethacrylate (UDMA) and Triethylene glycol dimethacrylate (TEGDMA) in (3:1) mass ratio [17, 18]. The UDMA-TEGDMA copolymer molecule contains 470 nuclei, 38 of them are Hydrogen. One can also use deuterized UDMA, where some of the Hydrogens are replaced by Deuterium atoms.

In the present theoretical model analysis we use the EPOCH kinetic model with Particle in Cell (PIC) method and the COMSOL Multiphysics model using the Finite Element Method (FEM), to solve the coupled Maxwell and Hydrodynamic equations.

2 Dynamics of the light-resonance in the nanorod

When a resonating nanoparticle of a size related to the effective wavelength of light is illuminated, a localised surface plasmon (LSP) is created. When the coherently oscillating electric field irradiates the metallic nanoparticle it causes the conduction electrons to oscillate also. The Coulomb attraction between electrons and nuclei produces a restoring force when the electron cloud is moved from its initial location. The electron cloud oscillates due to this force. The effective electron mass, the size and form of the charge distribution, and the electron density all contribute to the oscillation frequency. The LSP has two key effects: it dramatically increases electric fields near the nanoparticle's surface and it increases optical absorption at the plasmon resonance frequency. The geometry of the nanoparticle can also be used to adjust surface plasmon resonance [19, 20].

A recent kinetic theoretical study analyzed the resilience of nanorod antennas under a short laser pulse irradiation in vacuum [21]. Now we extend these studies to nanorod antennas embedded into the UDMA-TEGDMA copolymer. Here we consider the refractive index of UDMA-TEGDMA (n = 1.53) [18], which slows down the propagation of light. The short laser pulse is chosen to have a length needed to propagate across the target of $7 \cdot 3\,\mu\text{m} = 21\,\mu\text{m}$ thickness. The nanorods are orthogonal to the direction of laser irradiation in this model study. The conduction electrons show behavior of strongly coupled plasma [22]. The gold antennas are smaller than the half wavelength of the irradiated light. At optical frequencies the classical ideal half-wavelength dipole antenna scaling of rod with length $L = \lambda/2$ breaks down.

Here instead an effective wavelength needs to be considered [22]. When the nanorods are embedded into a surrounding medium different from vacuum the effective wavelength scales as follows:

$$\frac{\lambda_{eff}}{2R\pi} = 13.74 - 0.12[\varepsilon_\infty + \varepsilon_s 141.04]/\varepsilon_s \\ -\frac{2}{\pi} + \frac{\lambda}{\lambda_p} 0.12\sqrt{\varepsilon_\infty + \varepsilon_s 141.04}/\varepsilon_s \quad (1)$$

where $\varepsilon_\infty = 11$ is the dielectric function in the infinite frequency limit [23] and λ_p = 138 nm is the plasma wavelength for gold. The propagation velocity of light inside the medium is reduced to $c_s = c/\sqrt{\varepsilon_s}$, where $\varepsilon_s = n^2$. This is a good motivation for using PIC methods for studying this behavior. We used similar principles as described in [21], using the EPOCH computing package [24–26]. We considered nanorod antennas with partly ionised gold atoms with three conducting electrons per atom due to the extreme external field strength.

Initially electrons in the $\lambda_{eff}/2$ = 85 nm [15] nanorod antenna follow the phase of the laser irradiation with t = 2.65 fs period. With time electrons diffuse out of the nanorod, mainly at its two ends (Figure 1). The potential wall to UDMA keeping the electrons in the nanorod is apparently smaller than in the case of surrounding vacuum [21].

Simulation studies using the COMSOL Multi-physics Finite Element Method (FEM) package with many parameters found

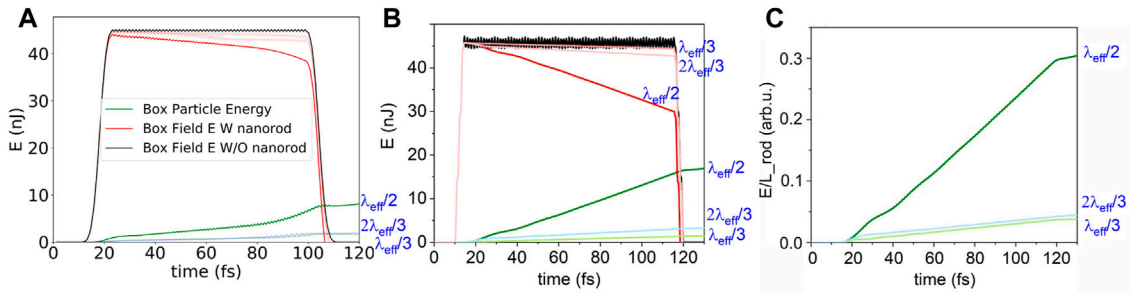

FIGURE 3
(color online) Optical response of the gold nanorod with different numerical methods and lengths, $L = \lambda_{eff}/2$, $\lambda_{eff}/3$ and $2\lambda_{eff}/3$, **(A)** PIC, **(B)** FEM and **(C)** FEM with normalized values to unit antenna length. The tendencies of the time-evolution of the nanorod energy determined by PIC and FEM are in very good agreement. The energy in the calculation box increases rapidly till about 20 fs, then it becomes constant (without nanoantenna) until the laser pulse lasts, at this moment the energy in the box drops to zero. With the nanoantenna in the box, the resonant antenna absorbs a good part of the laser energy, (green line), while much less with the non-resonant length antennas. There is a quantitative difference between the rates of energy increase, namely the slope is significantly smaller for PIC computations, accordingly the value achieved at 106 fs is also smaller. The smaller slope is caused by the tunneling of the electrons out of the antenna that is included into the PIC computations but not in FEM. The **(C)** figure shows that the difference between the two non-resonant antennas is caused by the antenna lengths, when this is removed by the length normalization the difference vanishes.

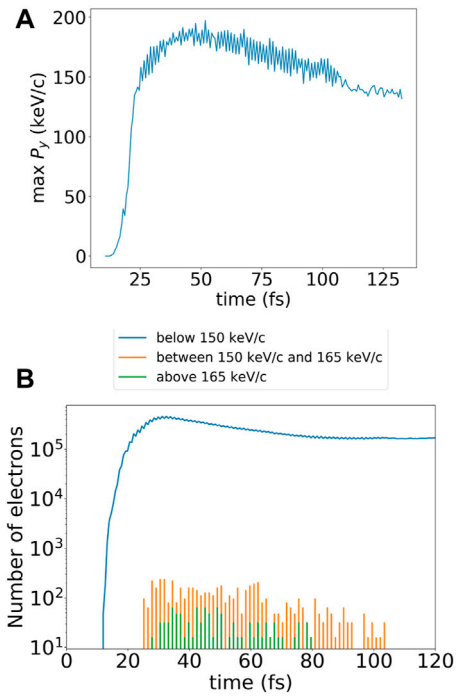

FIGURE 4
(color online) The behaviour of electrons leaving the nanorod. Flat plateau laser light reaches the nanorod with maximum intensity at around 20 fs and leaves the calculation box at 106 fs. Figure **(A)** indicates the maximum momentum in time reached by a spilled out electron in the y direction (direction of polarization of light in line with the nanorod's orientation in our simulations). Figure **(B)** shows the distribution of electrons at different momentum values: below 150 keV/c (blue line), above 150 keV/c (orange line) and above 165 kev/c (green line).

absorption coefficient between 256 cm^{-1} and 1,142 cm^{-1} for nanorod antennas [14]. By varying the density distribution of implanted nanoantennas one could achieve almost uniform integrated energy absorption at a given overlapping time of 240 fs for two counter-propagating 120 fs laser pulses [14, 27].

The beam intensity utilized was $I = 4 \cdot 10^{15} W/cm^2$ so that the plasmonic nanoantennas are not destroyed before the laser pulse passes. This damage threshold also depends on the geometry and size of the nanoantennas.

We compared the time dependence of momentum of escaping electrons in vacuum and in UDMA. The magnitude and the dynamics of electron emission is quite different, as shown in Figure 2.

Conduction band electrons follow the oscillating field, which results in nearfield enhancement [14], however in the process of repeated excitation the gold nanoparticles get ionized [28]. This leads to electron spill out effects [29]. The simulations shows faster electron spill-outs than the decrease of the plasmonic effect (see Figure 2).

For the emission of a single electron from gold plasmonic nanoantennas four 795 nm photons are needed. On the other hand the incoming pulse generates a surface plasmon, which may later emit electrons. This indirect process is more frequent than the direct emission by four photons [30–32].

Similarly to the analysis in Ref. [21] we now study the energy transfer dynamics from the laser irradiation to the target, with and without nanorods.

Consider now an intense laser beam (laser wave length $\lambda = 795$ nm in vacuum and 795/1.53 in UDMA), with intensity $I = 4 \cdot 10^{15} W/cm^2$, irradiating a calculation box (CB) of cross section $S_{CB} = 530 \cdot 530\ nm^2 = 2.81 \cdot 10^{-9}\ cm^2$ and of length $L_{CB} = \lambda = 795$ nm, with a step-function time profile of pulse length $T_P = 106$ fs ($\sim 40\lambda/c$). The laser pulse energy fraction falling into this box is $E_P = 1.19\ \mu J$. In the geometrical middle we insert a single nanorod antenna of length 85 nm and diameter 25 nm. As the calculation box size (λ) is 1.53·1/40th of the irradiation pulse length (40λ), the initial and final transients are negligible. See Figure 3.

We used two different marker particle species, 42,500 positively charged gold ions (+3) and three (127,500) conducting electrons for each, being careful to the neutral charge of the nanoantenna. We define the size of the nanorod, indicating the limits where the particle number density becomes zero. The borders of which can be seen in Figure 1.

We consider three situations, the box contains (i) vacuum, (ii) UDMA-TEGDMA copolymer and (iii) UDMA-TEGDMA copolymer with gold nanorod antenna in the middle of the box.

We consider the following processes for direct absorption to the UDMA-TEGDMA. As the copolymer is transparent the light absorption is minimal, while the refractive index is $n = 1.53$. The absorption coefficient of the bare polymer matrix at this wavelength would be $\approx 0.3\ cm^{-1}$ while doped with gold nanorods it would reach $18\ cm^{-1}$ [18].

In the EPOCH PIC kinetic plasma simulations model one is usually interested in charged particles, where the surrounding medium is vacuum. However, here we simulate metal nanoantenna with conducting electrons approached as plasma and the UDMA-TEGDMA copolymer is taken into account with a relative electric permittivity different from vacuum. The wavelength inside the simulation box containing UDMA-TEGDMA is also shrunk according to the refractive index.

3 Conclusion and outlook

The result of this simulation shows that the resilience of the nanoantenna in the UDMA-TEGDMA copolymer is similar to the vacuum case. In case of vacuum at 19 fs, when the maximum intensity of the laser reaches the nanorod, most electrons, $N_e = 10^3$, have 0.015 MeV/c momentum in the direction of polarization. However at the time when the irradiation finishes at 106 fs, around $N_e = 2 \times 10^2$ electrons remain at this momentum [21]. Other electrons escape at the tip of the nanorod. At 43 fs the number of leaving electrons reach the maximum while also achieving the maximum momentum in the direction of polarization (Figure 4). Potential difference becomes $E_y = +/- 2.9 \times 10^{12}$ V/m $= +/- 2.9 \times 10^3$ V/nm. Maximum momentum of leaving electrons in the direction of polarization reaches 0.3025 MeV/c in vacuum, in UDMA-TEGDMA at the same time the maximum is lower at 0.1799 MeV/c. The total momentum amplitude at this time is also lower in 4.5 GeV/c in UDMA-TEGDMA compared to 7.5 GeV/c in vacuum.

The decay time of the nanoantenna is longer in UDMA-TEGDMA, but it absorbs less energy due to its smaller resonant size (85 nm) compared to (130 nm) in Vacuum. The life-time of the plasmonic effect is starting shortly after the electron spill-out effects, around 25–30 fs later, however, short ignition is planned [1] and this time is enough in the UDMA-TEGDMA copolymer for the light to travel the required 6 μm.

Similar to [21] we also studied the time dependence of the momentum fluctuation of the electrons. Now the proton fluctuations were also studied. Initially the proton distribution slightly lags behind the electrons indicating that the electrons are pulling the protons. At later time as the laser drive is over the two distributions become aligned in phase. This phenomena will need further investigation.

The time dependence of the energy absorption by a nanorod in UDMA-TEGDMA copolymer was also studied in the COMSOL Multiphysics model. The results are similar, the main difference between the two models is arising from the different treatment of the conducting electrons. In the PIC model the conduction band electrons move freely and can escape leaving the gold ions behind, in the Maxwell-Hydrodynamic FEM approach the electrons' collective motion is taken into account indirectly through damping constants and they cannot leave from the surface of the nanorod.

Recent experimental tests on 150 μm thick nanorod filled polymer targets show a significantly increased crater volume accompnied by Deuterium outflow following laser irradiation pulses up to 25 mJ [33–36]. Therefore first continuation of this work, already in the making, is increasing the simulation box size and allowing more light-resonant nanord antennas and bringing the initial conditions closer in line with the crater formation experiments.

Data availability statement

The raw data supporting the conclusion of this article will be made available by the authors, without undue reservation.

Author contributions

LC and IP, conceived of the presented idea and took lead in writing the article. MC, AS, and DV, were responsible for simulations with comsol COMSOL and drawing figures. MC performed critical reading of the manuscript. TB and NK were managing and supervising the progect. LB, AK, and PR critical feedback and proof reading. HS and DS, were investigating and supervising the findings of this work. IM, AM, and LS investigated and verified the calculations. ÁS, JK, and AB, are synthesizing the polymer with gold nanorods and were responsible for measuring and calculating absorption and refraction index. AB also did critical reading and correcting. All authors discussed the results and contributed to the final manuscript.

Funding

This work is supported in part by the Frankfurt Institute for Advanced Studies, Germany, the Eötvös Loránd Research Network of Hungary, the Research Council of Norway, grand no. 255253, and the National Research, Development and Innovation Office of Hungary, via the projects: Nanoplasmonic Laser Inertial Fusion Research Laboratory (NKFIH-468-3/2021), Optimized nano-plasmonics (K116362), and Ultrafast physical processes in atoms, molecules, nanostructures and biological systems (EFOP-3.6.2-16-2017-00005).

Acknowledgments

Enlightening discussions with Johann Rafelski are gratefully acknowledged. HS acknowledges the Judah M. Eisenberg Professor Laureatus chair at Fachbereich Physik of Goethe Universität Frankfurt. We would like to thank the Wigner GPU Laboratory at the Wigner Research Center for Physics for providing support in computational resources. LC acknowledges support from Wigner RCP, Budapest (2022-2.2.1-NL-2022-00002).

Conflict of interest

HS was employed by the GSI Helmholtzzentrum für Schwerionenforschung GmbH.

The remaining authors declare that the research was conducted in the absence of any commercial or financial relationships that could be construed as a potential conflict of interest.

Publisher's note

References

1. Csernai LP, Csete M, Mishustin IN, Motornenko A, Papp I, Satarov LM, et al. Radiation-Dominated implosion with flat target. *Phys Wave Phenomena* (2020) 28(3): 187–99. (arXiv:1903.10896v3). doi:10.3103/s1541308x20030048

2. Chandrasekhar S. *Hydrodynamic and hydromagnetic stability*. Oxford, UK: Oxford U. Press (1961).

3. Kilkenny JD, Glendinning SG, Haan SW, Hammel BA, Lindl JD, Munro D, et al. A review of the ablative stabilization of the Rayleigh-Taylor instability in regimes relevant to inertial confinement fusion. *Phys Plasmas* (1994) 1(5):1379–89. doi:10.1063/1.870688

4. Cabot WH, Cook AW. Reynolds number effects on Rayleigh-taylor instability with possible implications for type-1a supernovae. *Nat Phys* (2006) 2:252.

5. Fukuda Y, Faenov AY, Tampo M, Pikuz TA, Nakamura T, Kando M, et al. Energy increase in multi-MeV ion acceleration in the interaction of a short pulse laser with a cluster-gas target. *Phys Rev Lett* (2009) 103:165002. doi:10.1103/physrevlett.103.165002

6. Boldarev AS, Gasilov VA, Faenov AY, Fukuda Y, Yamakawa K. Gas-cluster targets for femtosecond laser interaction: Modeling and optimization. *Rev Sci Instr* (2006) 77:083112. doi:10.1063/1.2336105

7. Rubovic P, Bonasera A, Burian P, Cao Z, Changbo F, Kong D, et al. Measurements of D-D fusion neutrons generated in nanowire array laser plasma using Timepix3 detector. *Nucl Instr Methods Phys Res Section A: Acc Spectrometers, Detectors Associated Equipment* (2021) 985:164680. doi:10.1016/j.nima.2020.164680

8. Ahn S, Choi J, Noh J, Cho SH. High aspect ratio nanoholes in glass generated by femtosecond laser pulses with picosecond intervals. *Opt Lasers Eng* (2018) 101:85–8. doi:10.1016/j.optlaseng.2017.10.002

9. Csernai LP. Detonation on timelike front for relativistic systems. *Sov Phys JETP* (1987) 65:219. School of Physics, University of Minnesota, Minneapolis, Minnesota, USA, Zh. Eksp. Teor. Fiz. 92, 397-386 (1987).

10. Csernai LP, Strottman DD. Volume ignition via time-like detonation in pellet fusion. *Laser Part Beams* (2015) 33:279–82. doi:10.1017/s0263034615000397

11. Csernai LP, Kroó N, Papp I. Radiation dominated implosion with nano-plasmonics. *Laser Part Beams* (2018) 36:171–8. doi:10.1017/s0263034618000149

12. Barbarino M. *Fusion reactions in laser produced plasma*. PhD thesis. College Station, TX: Texas A&M University (2015).

13. Zhang G, Huang M, Bonasera A, Ma YG, Shen BF, Wang HW, et al. Nuclear probes of an out-of-equilibrium plasma at the highest compression. *Phys Lett A* (2019) 383(19): 2285–9. doi:10.1016/j.physleta.2019.04.048

14. Csete M, Szenes A, Tóth E, Vass D, Fekete O, Bánhelyi B, et al. Comparative study on the uniform energy deposition achievable via optimized plasmonic nanoresonator distributions. *Plasmonics* (2022) 17(2):775–87. doi:10.1007/s11468-021-01571-x

15. Bonyár A, Borók A, Szalóki M, Petrik P, Csete M, Veres M, et al. (NAPLIFE collaboration), nanoplasmonic laser fusion target fabrication - considerations and preliminary results. *Int Conf New Front Phys Kolymbari, Crete, Greece, Sept.* (2020) 11.

16. Csete M, Vass D, Szenes A, Tóth E, Bánhelyi B, Papp I, et al. Plasmonic nanoresonator distributions for uniform energy deposition in active targets. *Opt Mater Express* (2022) 13:9. accepted for publication. doi:10.1364/OME.471980

17. Izabela M. Barszczewska-Rybarek Structure-property relationships in dimethacrylate networks based on Bis-GMA, UDMA and TEGDMA. *Dental Mater* (2009) 25(9):1082–9. doi:10.1016/j.dental.2009.01.106

18. Bonyár A, Szalóki M, Borók A, Rigó I, Kámán J, Zangana S, et al. The effect of femtosecond laser irradiation and plasmon field on the degree of conversion of a UDMA-TEGDMA copolymer nanocomposite doped with gold nanorods. *Int J Mol Sci* (2022) 23(21):13575. doi:10.3390/ijms232113575

19. Lance Kelly K, Coronado E. The optical properties of metal Nanoparticles: the influence of size, shape, and dielectric environment. *The J Phys Chem B* (2003) 107(3): 668–77. doi:10.1021/jp026731y

20. Maier SA. *Plasmonics: Fundamentals and applications*. New York, NY: Springer Science and Business Media (2007).

21. Papp I, Bravina L, Csete M, Kumari A, Mishustin IN, Molnár D, et al. Kinetic model evaluation of the resilience of plasmonic nanoantennas for laser-induced fusion. *PRX Energy* (2022) 1:023001. doi:10.1103/prxenergy.1.023001

22. Novotny L. EffectiveWavelength scaling for optical antennas. *Phys Rev Lett* (2007) 98:266802. doi:10.1103/physrevlett.98.266802

23. Dresselhaus MS. *Solid state physics - Part II optical properties of solids*. MIT Lecture Notes (2001).

24. Arber TD, Bennett K, Brady CS, Lawrence-Douglas A, Ramsay MG, Sircombe NJ, et al. Contemporary particle-in-cell approach to laser-plasma modelling. *Plasma Phys Control Fusion* (2015) 57:113001. doi:10.1088/0741-3335/57/11/113001

25. Nanbu K, Yonemura S. Weighted particles in coulomb collision simulations based on the theory of a cumulative scattering angle. *J Comput Phys* (1998) 145:639–54. doi:10.1006/jcph.1998.6049

26. Pérez F, Gremillet L, Decoster A, Drouin M, Lefebvre E. Improved modeling of relativistic collisions and collisional ionization in particle-in-cell codes. *Phys Plasmas*. (2012) 19(8):083104. doi:10.1063/1.4742167

27. Papp I, Bravina L, Csete M, Mishustin IN, Molnár D, Motornenko A, et al. Laser wake field collider. *Phys Lett A* (2021) 396:127245. doi:10.1016/j.physleta.2021.127245

28. Shoji M, Ken Miyajima MF, Mafuné F. Ionization of gold nanoparticles in solution by pulse laser excitation as studied by mass spectrometric detection of gold cluster ions. *The J Phys Chem C* (2008) 112(6):1929–32. doi:10.1021/jp077503c

29. Rivacoba A. Electron spill-out effects in plasmon excitations by fast electrons. *Ultramicroscopy* (2019) 207:112835. doi:10.1016/j.ultramic.2019.112835

30. Merschdorf M, Pfeiffer W, Thon A, Voll S, Gerber G. Photoemission from multiply excited surface plasmons in Ag nanoparticles. *Appl Phys A* (2000) 71:547–52. doi:10.1007/s003390000712

31. Farkas G, Horváth ZG. Multiphoton electron emission processes induced by different kinds of ultrashort laser pulses. *Opt Comm.* (1974) 12:392–5. doi:10.1016/0030-4018(74)90128-X

32. Farkas G, Horváth ZG, Tóth C. Linear surface photoelectric effect of gold in intense laser field as a possible high-current electron source. *J Appl Phys* (1987) 62:4545. doi:10.1063/1.339047

33. Archana Kumari, for the NAPLIFE Collaboration. LIBS analysis of pure, deuterated and Au-doped UDMA-TEGDMA mixture: A part of the nanoplasmonic laser fusion experiments. In: 11th Int. Conf. on New Frontiers in Physics; 7th Sept. 2022; Kolymbari, Crete, Greece (2022).

34. Miklós Veres, for the NAPLIFE Collaboration. Raman spectroscopic study of structural transformations in methacrylate polymer doped with plasmonic gold nanoparticles upon irradiation with high-energy femtosecond laser pulse. In: 11th Int. Conf. on New Frontiers in Physics; 7th Sept. 2022; Kolymbari, Crete, Greece (2022).

35. Norbert Kroó, for the NAPLIFE Collaboration (2022). High field nanoplasmonics and some applications—invited talk—Margaret Island Symposium 2022 on Vacuum Structure, Particles, and Plasmas. Budapest (Accessed May 15–18, 2022).

36. Péter Rácz, for the NAPLIFE Collaboration (2022). LIBS spectra from polymer shootings invited talk–Margaret Island Symposium 2022 on Vacuum Structure, Particles, and Plasmas. Budapest (Accessed May 15–18, 2022).